Platinum Ethyl Complexes with β-Agostic Pt–H–C Bonding†

Nicholas Carr,[a] Laura Mole,[b] A. Guy Orpen[a] and John L. Spencer*[,b]

[a] *Department of Inorganic Chemistry, University of Bristol, Cantock's Close, Bristol BS8 1TS, UK*

[b] *Department of Chemistry and Applied Chemistry, University of Salford, Salford M5 4WT, UK*

Protonation with non-co-ordinating acids of the complexes $[Pt(\eta^2\text{-}C_2H_4)(L\text{–}L)]$ [L–L = $(H_{11}C_6)_2P(CH_2)_2P(C_6H_{11})_2$, **1a**, $Bu^t_2P(CH_2)_2PBu^t_2$, **1b**, $(H_{11}C_6)_2P(CH_2)_3P(C_6H_{11})_2$, **1c**, $Bu^t_2P(CH_2)_3PBu^t_2$, **1d** or *o*-$Bu^t_2PCH_2C_6H_4CH_2PBu^t_2$, **1e**] and $[PtEt_2(L\text{–}L)]$ **2a–2d** affords a series of cationic platinum(II) complexes **3a–3e** which in the case of **3a–3c** adopt a *cis* ethene/hydride ground state whereas in **3d** and **3e** the otherwise electron-deficient metal centre is stabilized by a two-electron, three-centre agostic interaction with the β-CH bond of the ethyl ligand. Complexes **1–3** were characterized by ^1H, ^{13}C and ^{31}P NMR spectroscopy and for **2d** and **3d** by single-crystal X-ray crystallography. The influence of the chelating diphosphine ligand on the strength of the agostic bond was monitored by NMR spectroscopy. This revealed that the cations undergo two fluxional processes in solution: (*a*) agostic methyl rotation and (*b*) β-elimination/ethene rotation, a combination of which scrambles all five protons and both carbon atoms of the 'C_2H_5' moiety. The ^{31}P nuclei, however, remain inequivalent at temperatures up to 300 K. The agostic interaction was displaced by a small two-electron donor molecule L to form the series of adducts $[PtEt(L)(L\text{–}L)]^+$ (L = acetonitrile or pyridine) in which the 'normal' ethyl complex is the first formed species. The adducts are unstable to loss of C_2H_4 by β-elimination to form the series of cationic hydrides $[PtH(L)(L\text{–}L)]^+$. For comparison, the complex $[PtH(O_3SCF_3)\{Bu^t_2P(CH_2)_3PBu^t_2\}]$ was synthesised and characterized by ^1H and ^{31}P NMR spectroscopy and X-ray crystallography.

The pathway followed by the β-elimination/alkene insertion reaction can be modelled by complexes with three-centre, two-electron M–H–C_β (β-agostic) interactions. Many complexes in which the agostic interaction is present in the ground state have been shown to exist and the area has recently been reviewed by Brookhart *et al.*[1] As part of our research into the factors which influence the position of the agostic alkyl *versus* the alkene/hydride equilibrium we have previously shown[2] that ancillary diphosphine ligands play a crucial role. In the series of complexes $[Pt(C_7H_{11})(L\text{–}L)]^+$ (C_7H_{11} = norbornyl, L–L = chelating diphosphine) the diphosphine ligands with the more bulky substituents (Bu^t against cyclohexyl) and large chelate ring size result in weaker Pt–H–C agostic interactions. In all cases studied however the agostic isomer was always preferred over the alkene/hydride form.

We now report a series of platinum-diphosphine complexes of the general type $[PtEt(L\text{–}L)]^+$ in which the preferred geometry of the complex is under the control of the associated diphosphine ligands. A preliminary report of this work has been published.[3]

Results and Discussion

The complexes $[Pt(\eta^2\text{-}C_2H_4)(L\text{–}L)]$ [L–L = $(H_{11}C_6)_2P(CH_2)_2P(C_6H_{11})_2$ (dcpe) **1a**, $Bu^t_2P(CH_2)_2PBu^t_2$ (dbpe) **1b**, $(H_{11}C_6)_2P(CH_2)_3P(C_6H_{11})_2$ (dcpp) **1c**, $Bu^t_2P(CH_2)_3PBu^t_2$ (dbpp) **1d** or *o*-$Bu^t_2PCH_2C_6H_4CH_2PBu^t_2$ (dbpx) **1e**], prepared by the reaction of $[Pt(cod)_2]$ (cod = cycloocta-1,5-diene) with diphosphines in the presence of C_2H_4 in hexane (Scheme 1), have been characterized by microanalysis and NMR (^1H, ^{13}C and ^{31}P) spectroscopy (Tables 1 and 2, and Experimental section). Compounds **1a** and **1c** have been prepared previously by a different method[4] but no NMR data were published. The ethene protons of the compounds give rise to signals in the ^1H NMR spectra at δ 1.45–2.20 with J(PtH) of about 57 Hz; the

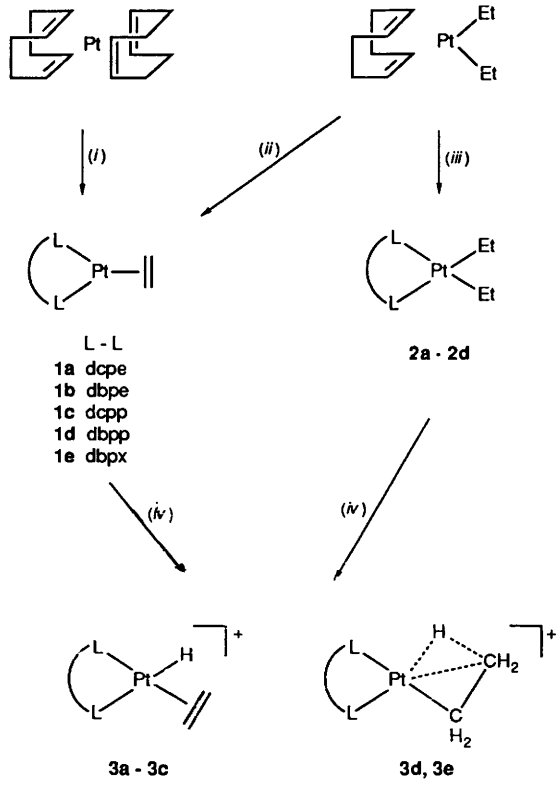

Scheme 1 (*i*) Diphosphine, 1 atm C_2H_4 (101 325 Pa), hexane, 273 K; (*ii*) dbpx, toluene, 373 K; (*iii*) diphosphine, diethyl ether at 293 K (**2a**, **2c**) or toluene at 363 K (**2b**, **2d**); (*iv*) HX, diethyl ether, 273 K

$^{13}C\text{-}\{^1H\}$ spectra show a characteristic signal for the carbons of the co-ordinated ethene at δ *ca.* 25, with coupling to ^{195}Pt [J(PtC) *ca.* 225 Hz]. The $^{31}P\text{-}\{^1H\}$ NMR spectra all show a single resonance with coupling to ^{195}Pt of 3100–3550 Hz. As a

† *Supplementary data available:* see Instructions for Authors, *J. Chem. Soc., Dalton Trans.*, 1992, Issue 1, pp. xx–xxv.

means of obtaining maximum information from NMR spectra, the synthesis of the doubly labelled [^{13}C]ethene analogue of **1b** was undertaken. The carbon atoms of the C_2H_4 ligand resonate in the ^{13}C-{^1H} NMR spectrum at the same chemical shift as for **1b** but the second-order AA'XX' spin system is apparent from which ^1J(CC) 36 Hz is obtained. This value is substantially reduced from the value for unco-ordinated ethene (67 Hz)[5] but is consistent with an η^2-bound ethene complex.[6] The proton-coupled ^{13}C NMR spectrum gives a value of ^1J(CH) of 130 Hz.

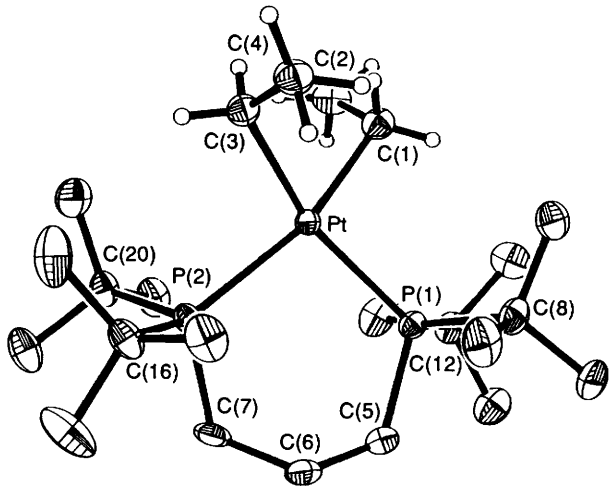

Fig. 1 Molecular structure of [$PtEt_2$(dbpp)] **2d**; all the dbpp hydrogen atoms have been omitted for clarity

The complexes [$PtEt_2$(L–L)] (L–L = dcpe **2a**, dbpe **2b**, dcpp **2c** or dbpp **2d**), prepared by treatment of [Pt(cod)Et_2] with diphosphines in Et_2O or toluene, have been characterized by NMR (^1H, ^{13}C and ^{31}P), microanalysis (see Table 1 and Experimental section) and in the case of **2d** by an X-ray crystallographic study. It was noteworthy that the attempted synthesis by this method of the analogous platinum diethyl complex with dbpx resulted in the isolation of [Pt(η^2-C_2H_4)(dbpx)], formed presumably by β-elimination and subsequent reductive elimination of C_2H_6 from the intermediate [$PtEt_2$(dbpx)]. The NMR spectra of the compounds **2a**–**2d** are consistent with their formulation as platinum(II) diethyl complexes (Table 3).

Protonation of the complexes [Pt(η^2-C_2H_4)(L–L)] **1a**–**1e** and [$PtEt_2$(L–L)] **2a**–**2d** with HBF_4·OEt_2 in diethyl ether at 273 K affords the off-white microcrystalline complexes **3a**–**3e** in 80–90% yield. The complexes **3d** and **3e** were also prepared as the PF_6^-, $CF_3SO_3^-$, $CPh(CF_3SO_2)_2^-$ and $CB_{11}H_{12}^-$ salts by protonation in the same way using the acids HPF_6, CF_3SO_3H, $CHPh(CF_3SO_2)_2$ and $HCB_{11}H_{12}$ respectively. The complex [PtH(O_3SCF_3)(dbpp)] **4**, which was isolated by treatment of **2d** with triflic acid (CF_3SO_3H) in the absence of ethene, is readily converted into **3d** by treatment with ethene.

Variable-temperature NMR studies (see Tables 4–6) on the complexes **3b**–**3e** (**3a** is unstable above 240 K) show that at temperatures above 240 K facile scrambling within the C_2H_5 moiety results in the equivalence of all five protons and both carbon atoms (but not the phosphorus atoms) such that sharp averaged signals are observed in the ^1H and ^{13}C NMR spectra. For example, the ^{13}C NMR spectrum of **3e** at 298 K shows a single resonance at δ 16.5 coupled to only one phosphorus nucleus but five hydrogen nuclei [J(PC) 18, J(CH) 67 Hz]. These observations are consistent with rapid intramolecular processes involving both the alkyl isomer in which methyl rotation is rapid and the ethene hydride form for which ethene rotation is rapid. However, the observation that the phosphorus environments always remain distinct in the NMR spectra implies that either methyl-group rotation occurs in place *via* a double agostic bond thus maintaining the integrity of the quasi-square-planar geometry, or that no pivoting of the ethyl

Table 1 Analytical data[a] and yields for the compounds [Pt(η^2-C_2H_4)(L–L)] **1**, [$PtEt_2$(L–L)] **2**, [PtH(η^2-C_2H_4)(L–L)]BF_4 **3a**–**3c** and [PtEt(L–L)]BF_4 **3d** and **3e**

		Analysis (%)		
Complex	L–L	C	H	Yield (%)
1b	dbpe	43.9 (44.4)	8.1 (8.2)	79
1d	dbpp	45.3 (45.4)	8.3 (8.35)	82
1e	dbpx	50.5 (50.6)	7.9 (7.8)	89
2a	dcpe	53.3 (53.2)	8.7 (8.6)	96
2b	dbpe	46.2 (46.2)	8.7 (8.8)	69
2c	dcpp	53.9 (54.0)	8.7 (8.8)	69
2d	dbpp	46.9 (47.2)	9.0 (9.0)	85
3a	dcpe	*b*		85
3b[c]	dbpe	36.3 (35.3)	6.9 (6.7)	87
3c	dcpp	*b*		85
3d	dbpp	38.8 (39.2)	7.4 (7.4)	80
3e[d]	dbpx	43.8 (43.3)	5.3 (5.4)	80

[a] Calculated figures in parentheses. [b] No accurate analyses were obtained because the salts are temperature sensitive. [c] As a CH_2Cl_2 solvate. [d] Analysis obtained for the $CPh(CF_3SO_2)_2^-$ salt.

Table 2 Selected room-temperature NMR data[a] (^{31}P, ^1H and ^{13}C) for the complexes [Pt(η^2-C_2H_4)(L–L)] **1a**–**1e**

Complex	δP[b]	J(PtP)	δH[c]	J(PH)	J(PtH)	δC[c,d]	J(PC)	J(PtC)
1a	70.4	3135	1.45	2	58	21.9	31	231
1b	101.6	3233	1.66	2	58	23.9	31	230
1c	24.3	3256	*e*			23.6	27	220
1d	47.2	3348	2.20[f]	2	56	26.6	27	219
1e	49.6	3551	2.18	2	57	27.2	28	217

[a] All data in CD_2Cl_2 unless otherwise stated. Chemical shifts in ppm, coupling constants in Hz. [b] Proton decoupled, chemical shifts are relative to $P(OPh)_3$ (δ 126.5). [c] Refers to the protons and carbon atoms of the C_2H_4 ligand. [d] Proton decoupled, chemical shifts are positive to high frequency of $SiMe_4$ (δ 0.0). [e] Obscured by diphosphine signals. [f] Measured in C_6D_6.

Table 3 Selected NMR data[a] (^{31}P, ^1H and ^{13}C) recorded at 298 K for the complexes [$PtEt_2$(L–L)] **2a**–**2d**. All measurements in C_6D_6

Complex	δP[b]	J(PtP)	δH[c]	J(PtH)	δC_α	$J(C_\alpha P_t)$	$J(C_\alpha P_c)$	$J(PtC_\alpha)$	δC_β	$J(PtC_\beta)$
2a	58.1	1641	1.95	72	10.9	*d*	*d*	*d*	16.9	*d*
2b	74.1	1575	1.84	70	7.6	100	9	674	16.7	21
2c	4.5	1700	*e*	—	11.0	98	11	*d*	16.8	23
2d	18.3	1634	1.45	72	11.1	97	10	692	17.2	23

[a] Chemical shifts in ppm, coupling constants in Hz. [b] Proton decoupled, chemical shifts are relative to $P(OPh)_3$ (δ 126.5). [c] For the H_α protons on the ethyl moiety only. [d] Not observed. [e] Obscured by diphosphine signals.

Table 4 Selected NMR (^{1}H, ^{13}C and ^{31}P) data[a] for complexes **3b–3e**

Complex	δP^1[b]	$J(PtP^1)$	δP^2	$J(PtP^2)$	δH[c]	$J(PH)$	$J(PtH)$	δC[d]	$J(PC)$	$J(PtC)$	$J(CH)$
3b	104.8	2965	90.6	2980	1.70	22	63	47.8	13	54	
3c	18.4	2833	12.8	3318	*e*			46.5	15	68	65
3d	38.1	2707	48.4	4919	0.77	13	65	15.9	18	91	67
3e	38.0	2800	53.2	5220	0.74	12	*f*	16.5	18	91	67

[a] Chemical shifts in ppm, coupling constants in Hz. Recorded at ambient temperature in CD_2Cl_2. No data available for complex **3a** which is unstable above −40 °C. [b] Proton decoupled, chemical shifts are relative to $P(OPh)_3$ (δ 126.5); P^1 is that phosphorus *cis* to the hydridic hydrogen, P^2 that *trans*. [c] Refers to the five protons of the ethyl moiety. [d] Proton decoupled; chemical shifts are positive to high frequency of $SiMe_4$ (δ 0.0). Refers to the two carbon atoms of the ethyl moiety. [e] Obscured by the diphosphine signals. [f] Not observed.

Table 5 Selected ^{1}H and ^{31}P NMR data[a] for complexes **3a–3e** recorded in CD_2Cl_2 at the temperature shown

Complex	*T*/K	δP^1[b]	$J(PtP^1)$	δP^2	$J(PtP^2)$	δH[c]	$J(PH)$	$J(PtH)$
3a	193	81.6	2976	69.9	2076	−3.2	115	690
3b	186	106.3	2971	91.5	2645	−4.6	109	508
3c	180	13.8	2925	6.7	2988	−4.2	94	423
3d	186	36.8	2680	47.4	4923	−2.6[d]	*e*	
3e	203	34.5	2778	50.0	5123	−2.8	*e*	

[a] Chemical shifts in ppm, coupling constants in Hz. [b] Proton decoupled, chemical shifts are relative to $P(OPh)_3$ (δ 126.5); P^1 is that phosphorus *cis* to the hydridic hydrogen; P^2 that *trans*. [c] Refers to the hydridic hydrogen or agostic hydrogen. [d] Recorded at 163 K in CD_2Cl_2–[$^2H_8$]tetrahydrofuran. [e] Not observed.

Table 6 Low-temperature ^{13}C NMR data[a] for the complexes [PtH($^{13}C_2H_4$)(dbpe)] **3b**, [Pt($^{13}C_2H_5$)(dbpp)] **3d** and [Pt($^{13}C_2H_5$)(dbpx)] **3e**

Complex	*T*/K	δC_α	$J(C_\alpha H)$	$J(C_\alpha C_\beta)$	$J(PC_\alpha)$	$J(PtC_\alpha)$	δC_β	$J(C_\beta H_{ag})$	$J(C_\beta H_t)$
3b	180	51.0[b]	160						
3d	145	22.0	158	26	41	200	8.2	60	153
3e	145	22.0	155	29	39	218	9.0	75	155

[a] In ppm with coupling constants in Hz; chemical shifts are positive to high frequency of $SiMe_4$ (δ 0.0). [b] One signal for both carbon nuclei.

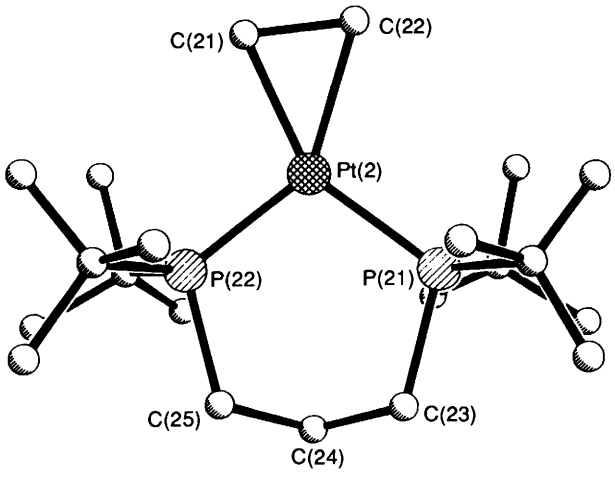

Fig. 2 Molecular structure of the major orientation of one of the two unique cations of [PtEt(dbpp)][$CB_{11}H_{12}$] **3d**. All hydrogen atoms of the dbpp have been omitted for clarity

group in a 14-electron species *via* a 'Y'-shaped intermediate occurs within the temperature range at which NMR spectra were recorded. The latter is contrary to the calculations of Thorn and Hoffmann[7] in which a low activation energy was assigned to this process. However, the ^{31}P NMR spectrum of **3e** at 298 K shows that the signals are broad which may imply that the ethyl group pivoting is becoming rapid at this temperature.

Parameters derived from the limiting ^{13}C NMR spectra (at 145 K), in particular ^1J(CH), show that for complexes **3d** and **3e** the evidence is consistent with the presence of ethyl ligands bound to platinum through both σ-alkyl and β-agostic C–H–Pt bonds. For example, in **3e**, C_α resonates at δ 22.0 as a triplet [^1J(CH) 155 Hz] whereas C_β at δ 9.0 has a triplet of doublets structure [^1J(CH) 155 and 75 Hz].

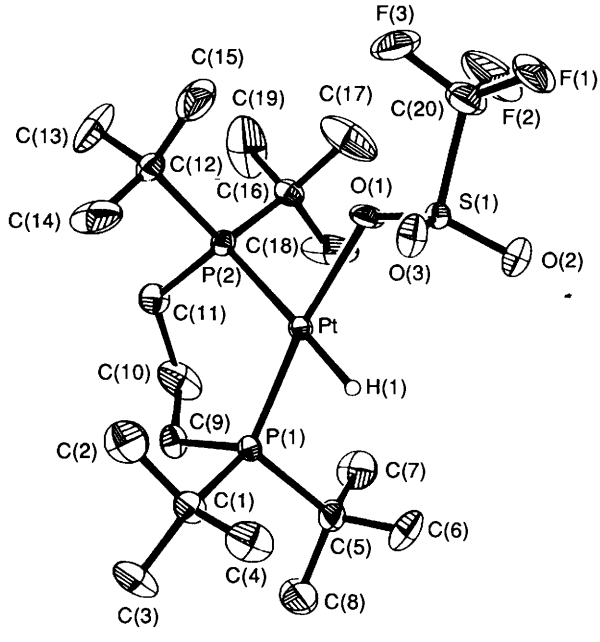

Fig. 3 Molecular structure of [PtH(O_3SCF_3)(dbpp)] **4**

The NMR evidence was borne out by a low-temperature X-ray crystallographic study on the $CB_{11}H_{12}^-$ salt of **3d**, [PtEt(dbpp)][$CB_{11}H_{12}$]; for comparison the structures of its diethyl precursor **2d** and the hydride complex [PtH(O_3SCF_3)-(dbpp)] **4** were also determined. Selected bond lengths and angles for the three structures are given in Table 7, the molecular geometries are shown in Figs. 1, 2 and 3, and the crystallographic data are summarized in Table 8. In all three structures the molecular species present are well separated, without strong intermolecular interactions. For **3d** there are

Table 7 Selected bond lengths (Å) and angles (°) for $[PtEt_2(dbpp)]$ **2d**, $[PtEt(dbpp)][CB_{11}H_{12}]$ **3d** and $[PtH(O_3SCF_3)(dbpp)]$ **4**

Compound **2d**

Pt–P(1)	2.329(2)	Pt–P(2)	2.320(2)
Pt–C(1)	2.103(10)	Pt–C(3)	2.113(9)
P(1)–C(5)	1.849(9)	P(1)–C(8)	1.901(8)
P(1)–C(12)	1.910(8)	P(2)–C(7)	1.868(9)
P(2)–C(16)	1.912(8)	P(2)–C(20)	1.897(8)
C(1)–C(2)	1.502(13)	C(5)–C(6′)	1.463(27)
C(3)–C(4)	1.494(12)	C(6)–C(7)	1.447(30)
C(5)–C(6)	1.523(16)	C(8)–C(10)	1.518(12)
C(6)–C(7)	1.549(16)	C(12)–C(13)	1.534(12)
C(8)–C(9)	1.520(12)	C(12)–C(15)	1.532(12)
C(8)–C(11)	1.527(11)	C(16)–C(18)	1.541(13)
C(12)–C(14)	1.514(11)	C(20)–C(21)	1.547(11)
C(16)–C(17)	1.520(11)	C(20)–C(23)	0.546(11)
C(16)–C(19)	1.503(12)		
C(20)–C(22)	1.509(12)		
P(2)–Pt–P(1)	97.9(1)	C(1)–Pt–P(1)	93.0(3)
C(1)–Pt–P(2)	160.0(2)	C(3)–Pt–P(1)	159.5(2)
C(3)–Pt–P(2)	94.0(3)	C(3)–Pt–C(1)	80.9(4)
C(5)–P(1)–Pt	116.6(3)	C(8)–P(1)–Pt	106.7(3)
C(8)–P(1)–C(5)	101.3(4)	C(12)–P(1)–Pt	121.6(3)
C(12)–P(1)–C(5)	98.7(4)	C(12)–P(1)–C(8)	110.1(4)
C(7)–P(2)–Pt	114.8(3)	C(16)–P(2)–Pt	121.9(3)
C(16)–P(2)–C(7)	100.2(4)	C(20)–P(2)–Pt	106.8(3)
C(20)–P(2)–C(7)	101.2(4)	C(20)–P(2)–C(16)	110.2(4)
C(2)–C(1)–Pt	110.0(7)	C(4)–C(3)–Pt	110.6(6)

Compound **3d**

Pt(1)–P(11)	2.295(4)	Pt(1)–P(12)	2.274(4)
Pt(1)–C(11)	2.068(25)	Pt(1)–C(12)	2.257(19)
Pt(2)–P(21)	2.257(6)	Pt(2)–P(22)	2.194(6)
Pt(2)–C(21)	2.092(25)	Pt(2)–C(22)	2.282(21)
P(11)–C(13)	1.811(14)	P(11)–C(16)	1.904(19)
P(11)–C(110)	1.897(16)	P(12)–C(15)	1.813(15)
P(12)–C(114)	1.824(20)	P(12)–C(118)	1.898(21)
P(21)–C(23)	1.953(18)	P(21)–C(26)	1.925(18)
P(21)–C(210)	1.859(20)	P(22)–C(25)	1.933(16)
P(22)–C(214)	1.855(21)	P(22)–C(218)	1.871(20)
C(11)–C(12)	1.469(43)	C(13)–C(14)	1.524(20)
C(14)–C(15)	1.511(20)	C(16)–C(17)	1.552(34)
C(16)–C(18)	1.580(27)	C(16)–C(19)	1.521(34)
C(110)–C(111)	1.436(25)	C(110)–C(112)	1.515(29)
C(110)–C(113)	1.545(24)	C(114)–C(115)	1.584(26)
C(114)–C(116)	1.596(28)	C(114)–C(117)	1.587(26)
C(118)–C(119)	1.548(30)	C(118)–C(120)	1.539(29)
C(118)–C(121)	1.473(26)	C(21)–C(22)	1.563(36)
C(23)–C(24)	1.538(21)	C(24)–C(25)	1.510(21)
C(26)–C(27)	1.429(26)	C(26)–C(28)	1.449(31)
C(26)–C(29)	1.522(24)	C(210)–C(211)	1.573(28)
C(210)–C(212)	1.516(30)	C(210)–C(213)	1.547(27)
C(214)–C(217)	1.565(27)	C(214)–C(216)	1.536(29)
C(214)–C(217)	1.591(36)	C(218)–C(219)	1.532(26)
C(218)–C(220)	1.514(25)	C(218)–C(221)	1.581(33)
P(11)–Pt(1)–P(12)	100.4(2)	P(11)–Pt(1)–C(11)	156.4(7)
P(12)–Pt(1)–C(11)	102.7(7)	P(11)–Pt(1)–C(12)	117.3(9)
P(12)–Pt(1)–C(12)	142.1(9)	C(11)–Pt(1)–C(12)	39.4(12)
P(21)–Pt(2)–P(22)	104.8(2)	P(21)–Pt(2)–C(21)	151.3(7)
P(22)–Pt(2)–C(21)	103.7(7)	P(21)–Pt(2)–C(22)	109.7(6)
P(22)–Pt(2)–C(22)	144.9(6)	C(21)–Pt(2)–C(22)	41.6(9)
Pt(1)–P(11)–C(13)	113.8(5)	Pt(1)–P(11)–C(16)	109.4(7)
C(13)–P(11)–C(16)	102.1(9)	Pt(1)–P(11)–C(110)	113.9(6)
C(13)–P(11)–C(110)	105.1(7)	C(16)–P(11)–C(110)	111.9(8)
Pt(1)–P(12)–C(15)	114.3(5)	P(1)–P(12)–C(114)	110.2(7)
C(15)–P(12)–C(114)	103.5(8)	Pt(1)–P(12)–C(118)	112.1(7)
C(15)–P(12)–C(118)	107.7(8)	C(114)–P(12)–C(118)	108.6(9)
C(15)–P(21)–C(23)	112.2(5)	Pt(2)–P(21)–C(26)	113.3(6)
C(23)–P(21)–C(26)	99.4(8)	Pt(2)–P(21)–C(210)	116.3(7)
C(23)–P(21)–C(210)	100.3(9)	C(26)–P(21)–C(210)	113.2(9)
Pt(2)–P(22)–C(214)	117.0(8)	Pt(2)–P(22)–C(25)	114.2(5)
Pt(2)–P(22)–C(218)	114.1(7)	C(25)–P(22)–C(214)	99.7(10)
C(214)–P(22)–C(218)	111.4(9)	C(25)–P(22)–C(218)	97.9(9)
Pt(1)–C(12)–C(11)	63.3(12)	Pt(1)–C(11)–C(12)	77.2(14)
Pt(2)–C(22)–C(21)	62.7(12)	Pt(2)–C(21)–C(22)	75.7(13)

Table 7 (*continued*)

Compound **4**

Pt–P(1)	2.201(3)	Pt–P(2)	2.374(3)
Pt–O(1)	2.181(9)	Pt–H(1)	1.64(10)
P(1)–C(1)	1.881(13)	P(1)–C(5)	1.908(13)
P(1)–C(9)	1.826(13)	P(2)–C(11)	1.852(14)
P(2)–C(12)	1.900(12)	P(2)–C(16)	1.904(13)
S–O(1)	1.461(11)	S–O(2)	1.409(8)
S–O(3)	1.418(11)	S–C(20)	1.788(17)
F(1)–C(20)	1.329(23)	F(2)–C(20)	1.311(24)
F(3)–C(20)	1.333(24)	C(1)–C(2)	1.530(20)
C(1)–C(3)	1.512(18)	C(1)–C(4)	1.539(21)
C(5)–C(6)	1.505(26)	C(5)–C(7)	1.508(25)
C(5)–C(8)	1.528(22)	C(9)–C(10)	1.448(20)
C(10)–C(11)	1.531(23)	C(12)–C(13)	1.525(23)
C(12)–C(14)	1.495(22)	C(12)–C(15)	1.468(22)
C(16)–C(17)	1.490(28)	C(16)–C(18)	1.443(27)
C(16)–C(19)	1.509(27)		
P(1)–Pt–P(2)	101.3(1)	P(1)–Pt–O(1)	170.2(3)
P(2)–Pt–O(1)	88.5(3)	P(1)–Pt–H(1)	80.8(36)
P(2)–Pt–H(1)	174.3(40)	O(1)–Pt–H(1)	89.5(36)
Pt–P(1)–C(1)	112.1(4)	Pt–P(1)–C(5)	112.5(4)
C(1)–P(1)–C(5)	110.5(6)	Pt–P(1)–C(9)	114.6(4)
C(1)–P(1)–C(9)	102.3(6)	C(5)–P(1)–C(9)	104.1(7)
Pt–P(2)–C(11)	112.1(4)	Pt–Pt(2)–C(12)	112.2(4)
C(11)–P(2)–C(12)	102.8(6)	Pt–P(2)–C(16)	112.6(4)
C(11)–P(2)–C(16)	104.0(6)	C(12)–P(2)–C(16)	112.5(6)

two independent cations in the crystal structure, which have similar geometries. The discussion below and the illustration in Fig. 2 refer to the major orientation of the better ordered of the two, that centred on Pt(2). The disorder present unfortunately limits the detail of the molecular geometry that may reliably be extracted for **3d**. In all three complexes the platinum is chelated by the dbpp ligand in the expected way. In **2d** the co-ordination of platinum is completed by two σ-ethyl ligands, in **3d** the platinum is bonded to just one ethyl ligand and does not interact with the anions (also disordered) which show the expected icosahedral shape. In **4** the platinum co-ordination is completed by a hydride ligand and an O-bonded trifluoromethanesulfonate ligand.

The solid-state structures of the cations of **3d**, although disordered, are similar to one another and consistent with the NMR spectra recorded at 145 K, in having the ethyl moiety bound asymmetrically to the platinum centre. The ethyl ligand bonds through a conventional σ-alkyl bond [Pt(2)–C(21) 2.09(3) Å] similar to those in the non-agostic ethyl ligands of **2d** [Pt–C 2.103(10), 2.113(9) Å], and a β-agostic interaction with the C–H bond of C_β [Pt(2)–C(22) 2.28(3) Å], although none of the ethyl hydrogen atoms could be located. The ethyl geometry is therefore similar to that observed in the agostic norbornyl complex[2] $[Pt(C_7H_{11})(dbpe)]BPh_4$ **5** [Pt–C_α 2.096(4) and Pt–C_β 2.309(5)]. The Pt–C_α–C_β angle in **3d** [75.7(13)°] is of course greatly reduced as compared with those of the non-agostic ethyls in **2d** [110.0(7), 110.6(6)°] but rather close to that [78.3(2)°] in **5**. While the C_α–C_β bond length in **3d** [1.56(4) Å] is poorly determined those of **2d** [1.494(12), 1.502(13) Å] provide a measure of the (librationally shortened) C–C distance prior to the distortions induced by the agostic interaction. The effect of such an interaction [as in **5**, C_α–C_β 1.480(6) Å] is typically to reduce the C–C bond length towards that expected for an η^2-bonded alkene. The hydride complex **4** provides a measure of the Pt–H interaction that is the logical extension of the agostic distortion of an ethyl (*i.e.* the completion of the partial β-elimination reaction that the agostic interaction represents). Thus the Pt–H distance in **4** [1.64(10) Å] may be compared to the Pt–H(C_β) distance in **5** [1.90(7) Å] and those in the non-agostic case of **2d** (> 3.06 Å).

These structures also provide information on the co-

Table 8 Crystallographic data * for complexes **2d**, **3d** and **4**

	2d	**3d**	**4**
Empirical formula	$C_{23}H_{52}P_2Pt$	$C_{22}H_{59}B_{11}P_2Pt$	$C_{20}H_{43}F_3O_3P_2PtS$
M	585.7	699.7	677.7
Crystal System	Monoclinic	Monoclinic	Orthorhombic
Space group	$P2_1/n$ (no. 14)	$P2_1/c$ (no. 14)	$Pna2_1$ (no. 33)
a/Å	11.661(3)	17.715(3)	23.383(7)
b/Å	15.394(3)	22.576(4)	8.663(1)
c/Å	14.915(2)	16.466(3)	13.987(3)
β/°	99.44(2)	90.046(13)	90
Z (molecules per cell)	4	8	4
U/Å^3	2641(1)	6584(2)	4503(2)
T/K	295	190	190
D_c/g cm^{-3}	1.47	1.41	1.61
μ(Mo-Kα)/cm^{-1}	54.6	44.1	52.2
Approximate crystal size/mm	0.5 × 0.5 × 0.6	0.50 × 0.30 × 0.25	0.6 × 0.5 × 0.3
2θ range/°	4–50	4–50	4–55
F(000)	1192	2832	1352
No. of data collected	5123	12 495	3115
No. of unique data	4677	11 665	2671
No. with $I > n\sigma(I)$, N_o	3373	6241	2113
n	3	2	3
Minimum, maximum transmission coefficients	0.128, 0.233	0.618, 0.922	0.267, 0.345
No. of variables, N_v	286	669	271
R	0.033	0.048	0.031
R'	0.040	0.056	0.040
S	1.28	1.47	1.25

* $R = \Sigma|\Delta|/\Sigma|F_o|$, $R' = (\Sigma w\Delta^2/\Sigma wF_o^2)^{\frac{1}{2}}$, $S = [\Sigma w\Delta^2/(N_o - N_v)]^{\frac{1}{2}}$, $\Delta = F_o - F_c$.

ordination geometry of the platinum atom under the small variations present. In each case the co-ordination may be loosely described as square planar, although there are significant deviations from planarity and the ligand set is not square (*i.e.* there is no C_4 axis of symmetry). This geometry is to be expected for the formal oxidation state of platinum present in each of complexes **2d**, **3d** and **4**. There are however some notable distortions present. Thus in **2d** the planes of the PtP_2 and PtC_2 units are twisted by 26.4° relative to one another (*cf.* a similar twist of 5.4° between the PtP_2 and PtHO planes in **4**). The P–Pt–P angles for the dbpp ligand are *ca.* 100° as judged from these structures [97.9(1), 104.8(2) and 101.3(1)° for **2d**, **3d** and **4** respectively] rather larger than for the dbpe ligand in **5** and the platinum(0) norbornene species [Pt(η^2-C_7H_{10})(dbpe)] [89.3(1) and 89.2(1)° respectively]. This confirms the expectation that the increased chelate ring size in these dbpp species is associated with a larger P–Pt–P angle. The Pt–P bond lengths in **2d**, **3d** and **4** show considerable variation which can be correlated with the *trans* ligand. Thus the Pt–P length *trans* to the weak ligand O_3SCF_3 in **4** is the shorter [2.201(3)], while the longer [2.374(3) Å] is *trans* to the hydride. The σ-alkyl carbons induce a Pt–P distance *ca.* 2.3 Å [2.320(2) and 2.329(2) in **2d**, 2.257(6) in **3d**, *cf.* 2.311(1) in **5**]. The Pt–P distance *trans* to the agostic interaction in **3d** is short [2.194(6), *cf.* 2.256(1) in **5**].

The strong dependence of both Pt–P bond length and J(Pt–P) on the *trans* ligand is clear. However there is an imperfect correlation between J(Pt–P) and the bond length, and clearly account must be taken of other factors (*cis* ligand, oxidation state, orbital effects, *etc.*). Similar comments apply to the Pt–C couplings and bond lengths. Interestingly the magnitudes of Pt–C_β couplings show very poor correlation with Pt • • • C_β distances, presumably because the factors dictating the coupling are complicated; for instance it is possible to envisage internuclear spin interaction by several routes.

The evidence from the NMR data (Tables 4–6) shows that the ground-state structures of complexes **3a**–**3c** are very different to those of **3d** and **3e**. For example, the ^{13}C NMR spectrum of **3b** at 180 K shows that the signal for the C_2 moiety is a triplet due to proton coupling with ^1J(CH) *ca.* 160 Hz as compared with ^1J(CH) 130 Hz for [Pt(η^2-$^{13}C_2H_4$)(dbpe)] and 157 Hz for unco-ordinated C_2H_4. Moreover, in the ^1H NMR spectra of **3a**–**3c** recorded at between 180 and 193 K (Table 5) there is a high-field signal in each case, typical of a hydride. For example in **3b** the hydride resonates at δ −4.6 with coupling to the *trans*-phosphorus atom and the platinum centre (109 and 508 Hz respectively). The IR spectrum of **3b** shows ν(PtH) at 2085 cm^{-1}. These observations are consistent with a *cis*-ethene/hydride ground-state structure for complexes **3a**–**3c** and may be compared with the similar hydride complex [PtH(O_3SCF_3)(dbpp)] **4** (see Experimental section) for which the hydride resonates at δ −6.6 with coupling to both *cis* and *trans* phosphorus nuclei [J(PH) 13 and 182 Hz respectively] and ^{195}Pt [J(PtH) 779 Hz].

Furthermore, inspection of the variable-temperature ^{31}P NMR data shows large differences in the values of ^1J(PtP) for the phosphorus nuclei *cis* and *trans* to the agostic bond in **3d** and **3e**, whereas for **3b** and **3c** at ambient temperatures the values for ^1J(PtP) are very similar to each other. The marked temperature dependence of ^1J(PtP) in **3b** and **3c** emphasizes the split in behaviour which occurs between **3b** and **3c** and the two agostic complexes **3d** and **3e**. Whereas both *cis*- and *trans*-^1J(PtP) for the latter vary little between the temperatures shown, the value of $^1J(PtP_{trans})$ for **3b** and **3c** decreases sharply from 298 to 180 K whilst $^1J(PtP_{cis})$ stays almost constant. One explanation of this behaviour is that at room temperature the values represent an average of contributions from each isomer in the equilibrium between agostic ethyl and ethene/hydride forms. At room temperature for **3a**–**3c** there may be present in solution significant concentrations of the agostic ethyl species which are in rapid equilibrium with the respective ethene/hydride isomers. As the temperature is lowered the thermodynamically preferred ethene/hydride complex dominates and is the only species present in observable concentration at the low-temperature limit.

For a series of cobalt complexes containing β-agostic interactions, Brookhart *et al.*[8] considered the possibility that there might be a continuum of bonding involving progressive transfer of hydrogen from the metal to the β-carbon. However, in the platinum complexes reported here this appears not to be the case and the alkene/hydride and agostic forms apparently represent energy minima separated by a small barrier. The presence of such a barrier could indicate that the lowest-energy

Table 9 Selected ^1H, ^{13}C and ^{31}P NMR[a] and IR data for the complexes $[PtEt(L)(L-L)]^+$ **6** (L = CD_3CN), **7** (L = C_5D_5N) and $[PtH(L)(L-L)]^+$ **8** (L = CD_3CN), **9** (L = C_5D_5N)

Complex	L–L	δP^1[b]	$J(PtP^1)$	δP^2	$J(PtP^2)$	δH[c]	$J(PtH)$	$J(P^1H)$	$J(P^2H)$	δC_α[d]	$J(PtC_\alpha)$	$J(PC_\alpha)$	$\nu(PtH)$[e]
6b	dbpe	87.7	1599	64.6	4415					6.8	453	81	
6d	dbpp	27.6	1561	21.2	4447					6.8	438	76	
6e[f]	dbpx	23.6	1565	19.7	4578					8.3	—	66	
7b	dbpe	79.1	1545	61.1	3839					9.5	490	83	
7d	dbpp	20.3	1506	16.9	3933					8.1	477	79	
8b	dbpe	91.5	1900	88.5	3945	−4.23	915	180	21				
8d	dbpp	29.0	1898	42.5	3923	−6.50	812	171	13				2086
8e	dbpx	28.1	2055	41.0	4103	−7.74	756	173	16				2128
9d	dbpp	24.0	1833	37.6	3498	−6.24	833	180	14				2095
9e	dbpx	26.3	2003	38.0	3670	−7.50	815	177	15				2119

[a] Chemical shifts in ppm, coupling constants in Hz, measurements at ambient temperature unless otherwise stated. [b] ^1H decoupled, chemical shifts are relative to $P(OPh)_3$ (δ 126.5 ppm). [c] Refers to the hydridic proton only. [d] ^1H decoupled; chemical shifts are positive to high frequency of $SiMe_4$ (δ 0.0 ppm). Refers to the C_α of the ethyl ligand. [e] Measured in CH_2Cl_2. [f] Measured at 215 K.

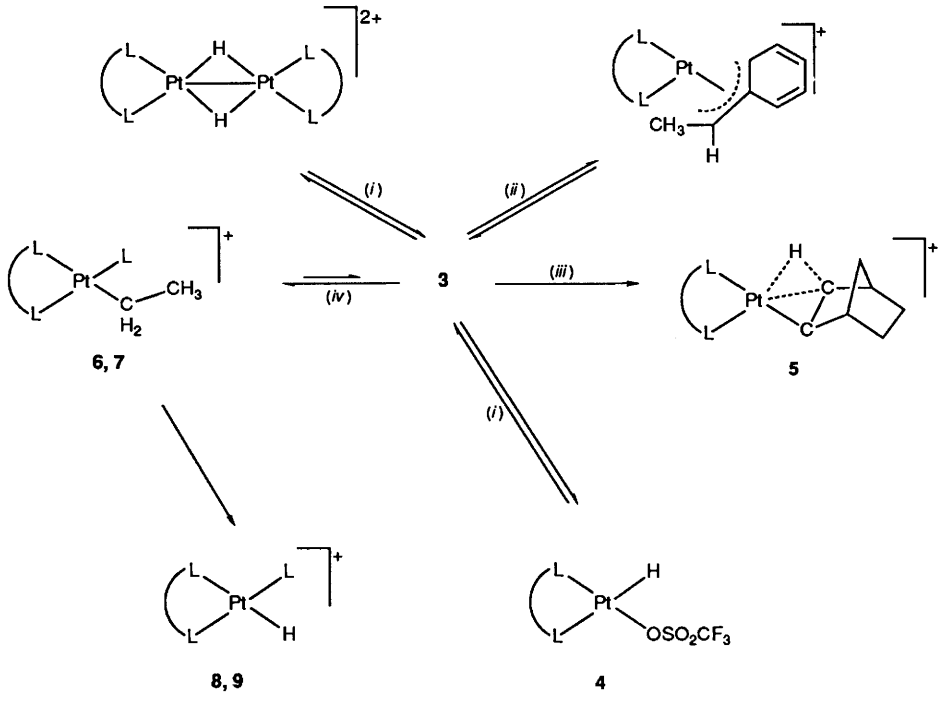

Scheme 2 (*i*) C_2H_4; (*ii*) styrene; (*iii*) norbornene; (*iv*) L = CD_3CN or C_5D_5N

ethene/hydride structure might be one in which the alkene lies perpendicular to the co-ordination plane of the complex as is observed in Zeise's salt, $K[PtCl_3(C_2H_4)]$. Unfortunately the NMR data recorded at the lowest accessible temperatures indicate that the alkene is still rotating rapidly and it is not therefore possible to distinguish between in-plane and perpendicular co-ordination of the alkene.

Considerable progress has already been made in assessing the influence of the chelating diphosphine ligands on the nature of the bonding in the complexes $[Pt(C_7H_{11})(L-L)]^+$,[2] for which it was clear that the agostic isomer was preferred for all the diphosphines used. In this series of diphosphine ethylplatinum(II) cations changes in the ancillary diphosphine ligands control the balance between the agostic ethyl and the ethene/hydride isomer. The control and understanding of this balance may prove critical in the chemistry of alkene polymerization and oligomerization reactions.

It is implicit in the results of our investigations that the smaller of the diphosphines favour the ethene/hydride isomer whilst the larger prefer the adoption of an agostic ethyl structure. The calculation of reaction pathways by molecular orbital theory has shown that[7] during the course of migration of a hydride to a co-ordinated ethene in a model complex $[PtH(\eta^2\text{-}C_2H_4)(PH_3)_2]^+$ the optimum ancillary ligands angle rises from 95 to 110° at the 'transition state' which would resemble a β-agostic species. Our results are consistent with this picture and demonstrate the crucial control which is exerted by the ancillary ligands on the degree of interaction between metal and the β-C–H agostic bond.

The series of cationic platinum(II) complexes **3a–3d** are unstable in dichloromethane solution with respect to loss of ethene to form the dinuclear cations $[Pt_2(\mu\text{-}H)_2(L-L)_2]^{2+}$. The complex $[PtEt(dbpx)]^+$ **3e** does not form a dinuclear cation by this pathway and it is of note that the diphosphine ligand in this complex has the largest bite angle of the diphosphines used which may render the corresponding dinuclear complex too sterically hindered to be stable. In the case of L–L = dbpp the agostic ethyl complex **3d** can be regenerated from the reaction of the dinuclear complex $[Pt_2(\mu\text{-}H)_2(dbpp)_2]^{2+}$ with C_2H_4. Loss of the C_2H_4 ligand from **3d** is facile in the presence of

norbornene or styrene to afford respectively $[Pt(C_7H_{11})(dbpp)]^+$ and the known η^3-benzyl complex[9] $[Pt(\eta^3\text{-}anti\text{-}1\text{-}MeCHPh)(dbpp)]^+$ (Scheme 2).

The displacement of the agostic interactions *via* nucleophilic attack at the metal in complexes **3d** and **3e** by the small two-electron donor molecules CD_3CN and C_5D_5N was investigated. The comparative reactivity of the ethene/hydride complex was also studied. NMR measurements of solutions of these complexes in CD_3CN and C_5D_5N showed the presence of the ethyl complexes **6b**, **6d**, **6e** and **7b**, **7d** which, with the exception of **7b**, are unstable towards β-elimination of C_2H_4 to form the series of cationic hydrides **8b**, **8d**, **8e** and **9d**, **9e** (see Scheme 2 and Table 9). Similar reactivity leading to displacement of the agostic bond by small two-electron donor ligands has been observed in, for example,[10,11] the compounds $[CoEt\{P(OMe)_3\}(\eta\text{-}C_5H_5)]^+$ and $[Co\{PPh_2(o\text{-}C_6H_4CHMe)\}(\eta\text{-}C_5H_5)]^+$.

Considerable progress has been achieved in assessing the influence of diphosphine ligand and alkyl on the position of the alkene/hydride *versus* agostic alkyl equilibrium, as monitored by NMR parameters. In particular it is clear that when the alkyl fragment is norbornyl the agostic isomer is always preferred (for all diphosphines used), whereas for 'ethyl' the less bulky, and smaller bite, diphosphines promote a predominance of the alkene/hydride isomer. The relief of ring strain in the norbornyl agostic isomer may be sufficient to favour this over the norbornene/hydride isomer with the smaller diphosphines. Alternatively the norbornene/hydride form may require more space than is offered even with the smallest phosphines used in this study. Within the norbornyl series the bulkier substituents (Bu^t *vs.* cyclohexyl) and larger chelate ring-size phosphines cause weaker agostic Pt–H–C interaction. The implications are that in platinum(II) diphosphine chemistry: (*i*) substituted alkyls (with β-hydrogens) are more easily accommodated in their agostic (η^2) form than as the corresponding alkene/hydrides; (*ii*) bulky, large chelate ring-size diphosphines promote the migration of hydride to alkene, increasingly favouring the alkyl over alkene/hydride form; and (*iii*) the degree of interaction between the β-C–H bond and platinum in agostic complexes is very precisely controlled by the nature of the ancillary diphosphine ligand.

Experimental

All reactions were carried out under a dry, oxygen-free nitrogen atmosphere using standard Schlenk-tube techniques. Solvents were thoroughly dried over the appropriate reagents and freshly distilled prior to use. The compounds $[Pt(cod)_2]$,[12] $[Pt(cod)Et_2]$,*[13] dbpe,[14] dcpp,[15] dbpe[2] and dbpx[16] were prepared by published methods; the compound dcpe was purchased from Strem Chemicals, the gas $^{13}C_2H_4$ from MSD isotopes. Analytical and other data are given in Table 1. The NMR spectra were recorded on a Bruker AC300 and IR spectra with a Perkin Elmer FT1710 spectrophotometer. Although not reported, all ^1H and ^{13}C NMR data showed the expected signals arising from the diphosphine ligands.

Synthesis of the Complexes.—$[Pt(\eta^2\text{-}C_2H_4)(L\text{–}L)]$ (L–L = dcpe **1a**, dbpe **1b**, dcpp **1c**, dbpp **1d** *or* dbpx **1e**]. The method used was identical for each complex. To a stirred solution of the diphosphine (0.15 g, *ca.* 0.4 mmol) in ethene-saturated hexane (20 cm^3) at 273 K was added an equimolar amount of $[Pt(cod)_2]$ over a period of *ca.* 10 min. After 30 min the solvent was removed *in vacuo* to afford the complexes as off-white *microcrystals*.

$[Pt(\eta^2\text{-}^{13}C_2H_4)(dbpe)]$. To a degassed frozen solution of $[Pt(cod)_2]$ (0.367 g, 0.9 mmol) and dbpe (0.298 g, 0.9 mmol) in hexane (25 cm^3) under vacuum at 77 K was condensed $^{13}C_2H_4$ (1.0 mmol, 92.1% by atom). After warming to ambient temperature and stirring for *ca.* 2 h the solvent was removed *in vacuo*. After purification by redissolving the reaction products in hexane (30 cm^3) and filtering off any undissolved material, the complex $[Pt(\eta^2\text{-}^{13}C_2H_4)(dbpe)]$ was obtained as off-white *crystals* the purity of which was checked by ^1H, ^{13}C and ^{31}P NMR spectroscopy.

$[PtEt_2(L\text{–}L)]$ (L–L = dcpe **2a** *or* dcpp **2c**). The synthesis of the two compounds was identical. A solution of the diphosphine (*ca.* 0.25 g, 0.6 mmol) in diethyl ether (10 cm^3) was treated with $[Pt(cod)Et_2]$ (*ca.* 0.21 g, 0.6 mmol). After 2 h the supernatant liquid was decanted and the precipitate dried *in vacuo* to reveal the complex as off-white *microcrystals*.

$[PtEt_2(L\text{–}L)]$ (L–L = dbpe **2b** *or* dbpp **2d**). A solution of the diphosphine (*ca.* 0.25 g, 0.8 mmol) and $[Pt(cod)Et_2]$ (*ca.* 0.29 g, 0.8 mmol) in toluene (5 cm^3) was heated to 363 K for 20 h. Reduction of the volume of solvent *in vacuo* to *ca.* 2 cm^3 and cooling to 250 K afforded colourless *crystals* of the complex.

$[Pt(\eta^2\text{-}C_2H_4)(dbpx)]$ **1e** *by an alternative method.* A solution of dbpx (0.39 g, 1 mmol) and an equimolar amount of $[Pt(cod)Et_2]$ in toluene (15 cm^3) was heated to 373 K for 20 h. The solvent was removed *in vacuo* to reveal complex **1e** as off-white *microcrystals*.

$[PtH(\eta^2\text{-}C_2H_4)(L\text{–}L)]X$ (X = BF_4, L–L = dcpe **3a**, dbpe **3b** *or* dcpp **3c**) *and* $[PtEt(L\text{–}L)]X$ [X = BF_4, PF_6, CF_3SO_3, $CPh(CF_3SO_2)_2$ *or* $CB_{11}H_{12}$; L–L = dbpp **3d** *or* dbpx **3e**]. The procedure was identical in each case. A solution of the diethyl or $\eta^2\text{-}C_2H_4$ complexes (*ca.* 0.3 g) in diethyl ether (10 cm^3) at 273 K was treated with an equimolar amount of $HBF_4{\cdot}OEt_2$ or $HBF_4{\cdot}OMe_2$ causing an immediate precipitate of a white solid. The supernatant liquid was decanted and the solid washed with diethyl ether (3 × 5 cm^3 portions). The precipitate was dried *in vacuo* to reveal the complex as off-white *microcrystals*. Complexes **1e** and **2d** were also protonated with other acids *viz.* HPF_6 (60% aqueous solution), CF_3SO_3H, $CHPh(CF_3SO_2)_2$[17] and $HCB_{11}H_{12}$.[18] The method was identical to that for $HBF_4{\cdot}OEt_2$ using equimolar amounts of the appropriate acid.

Table 10 Atomic coordinates (× 10^4) for complex **2d**

Atom	*x*	*y*	*z*
Pt	10 196(1)	2 244(1)	2 438(1)
P(1)	11 716(2)	1 308(1)	2 270(1)
P(2)	8 789(2)	1 199(1)	2 540(1)
C(1)	11 026(9)	3 324(7)	1 965(6)
C(2)	10 382(12)	3 608(7)	1 057(7)
C(3)	9 270(8)	3 246(6)	2 975(6)
C(4)	9 880(9)	3 512(7)	3 894(7)
C(5)	11 442(8)	134(6)	2 388(7)
C(6) [a]	10 433(12	−182(8)	2 834(10)
C(6′) [b]	10 273(25)	− 88(13)	1 927(21)
C(7)	9 223(8)	65(5)	2 302(6)
C(8)	12 909(7)	1 506(6)	3 281(5)
C(9)	13 268(8)	2 455(6)	3 376(6)
C(10)	12 409(8)	1 269(7)	4 127(6)
C(11)	13 998(7)	956(7)	3 274(7)
C(12)	12 361(7)	1 272(6)	1 173(5)
C(13)	13 144(9)	2 056(6)	1 082(6)
C(14)	11 344(8)	1 298(7)	399(5)
C(15)	13 074(8)	454(7)	1 065(6)
C(16)	8 171(8)	1 016(6)	3 636(6)
C(17)	9 168(8)	1 121(7)	4 423(5)
C(18)	7 260(8)	1 711(8)	3 764(6)
C(19)	7 608(10)	148(7)	3 720(7)
C(20)	7 566(7)	1 396(6)	1 554(5)
C(21)	8 129(8)	1 323(7)	688(5)
C(22)	7 051(8)	2 296(7)	1 545(7)
C(23)	6 595(8)	703(7)	1 467(6)

[a] Occupancy 0.64(1). [b] Occupancy 0.36(1).

* The method in ref. 13 was considered unsatisfactory as [Pt(cod)Et(Cl)] was produced as an impurity. It was modified by use of 2 equivalents of $ZnEt_2$ instead of MgEtBr and pure products were obtained consistently in good yield.

Table 11 Atomic coordinates (× 10^4) for complex **3d**

Atom	*x*	*y*	*z*	Atom	*x*	*y*	*z*
Pt(1)[a]	2542(1)	6792(1)	2425(1)	C(24′)[d]	2230	4822	7777
Pt(2)[b]	2491(1)	4307(1)	7551(1)	C(25′)[d]	2411	4709	6866
Pt(1′)[c]	2544(2)	5715(2)	2590(3)	C(26)	1906(9)	3563(9)	9304(11)
Pt(2′)[d]	2560(6)	3232(4)	7412(6)	C(27)	2138(10)	3983(8)	9904(10)
P(11)	2753(2)	6274(2)	3603(2)	C(28)	1737(12)	2975(10)	9607(13)
P(12)	2336(2)	6033(2)	1545(3)	C(29)	1187(9)	3773(11)	8888(10)
P(21)	2659(3)	3572(3)	8462(3)	C(210)	3635(11)	3471(10)	8854(14)
P(22)	2251(3)	3854(3)	6401(3)	C(211)	3882(8)	4106(8)	9148(9)
C(11)[a]	2527(13)	7525(10)	1673(16)	C(212)	3722(10)	3024(10)	9534(10)
C(12)[a]	2661(10)	7787(8)	2477(22)	C(213)	4154(8)	3320(10)	8127(10)
C(13)[a]	2782(8)	5479(6)	3464(9)	C(214)	2986(11)	3896(13)	5600(13)
C(14)[a]	2234(9)	5213(8)	2850(9)	C(215)	2756(10)	3655(9)	4744(9)
C(15)[a]	2478(9)	5303(6)	1979(9)	C(216)	3705(10)	3552(10)	5821(11)
C(11′)[c]	2424	4862	2269	C(217)	3202(12)	4571(10)	5455(14)
C(12′)[c]	2576	4928	3329	C(218)	1291(11)	4009(11)	5978(12)
C(13′)[c]	2629	7234	3152	C(219)	965(8)	3550(7)	5390(8)
C(14′)[c]	2792	7294	2224	C(220)	743(9)	4052(9)	6680(9)
C(15′)[c]	2207	7078	1597	C(221)	1289(13)	4630(10)	5534(15)
C(16)	3745(10)	6439(12)	3990(13)	B(11)	5532(12)	5380(12)	7670(16)
C(17)	4011(11)	5906(11)	4512(14)	B(12)	5127(12)	5594(9)	6691(13)
C(18)	4239(8)	6492(10)	3195(11)	B(13)	4431(11)	5483(11)	7523(15)
C(19)	3755(11)	7028(11)	4438(13)	B(14)	4888(11)	5630(8)	8436(11)
C(110)	2012(9)	6404(8)	4416(10)	B(15)	5818(13)	5936(12)	8198(17)
C(111)	2266(10)	6222(9)	5206(11)	B(16)	5935(12)	5978(13)	7222(17)
C(112)	1766(10)	7046(10)	4430(10)	B(17)	5681(13)	6588(9)	7679(17)
C(113)	1295(9)	6068(10)	4145(12)	B(18)	5290(21)	6434(14)	6754(20)
C(114)	3017(11)	6059(10)	716(12)	B(19)	4379(14)	6214(13)	6972(13)
C(115)	2851(9)	6511(7)	2(11)	B(110)	4260(11)	6193(9)	7982(12)
C(116)	3137(10)	5436(8)	279(10)	B(111)	5080(15)	6426(12)	8451(16)
C(117)	3833(9)	6230(9)	1040(11)	B(112)	4741(15)	6721(10)	7496(14)
C(118)	1349(11)	6054(9)	1097(15)	B(21)	−79(14)	6017(10)	6863(13)
C(119)	1218(12)	5537(9)	495(14)	B(22)	321(12)	5820(10)	7852(14)
C(120)	781(11)	5896(10)	1769(11)	B(23)	755(15)	6364(18)	7216(15)
C(121)	1082(9)	6615(6)	742(13)	B(24)	43(12)	6730(9)	6721(11)
C(21)[b]	2384(9)	5202(11)	7258(16)	B(25)	−784(16)	6480(13)	6992(17)
C(22)[b]	2501(11)	5201(9)	8199(15)	B(26)	−636(12)	5944(11)	7713(13)
C(23)[b]	2478(10)	2791(8)	7991(9)	B(27)	−854(10)	6656(8)	8109(11)
C(24)[b]	2676(9)	2698(7)	7091(9)	B(28)	−178(9)	6214(9)	8573(12)
C(25)[b]	2158(8)	3003(7)	6495(7)	B(29)	712(11)	6447(11)	8261(12)
C(21′)[d]	2408	2632	6632	B(210)	486(14)	7056(12)	7601(13)
C(22′)[d]	2625	2314	7568	B(211)	−387(10)	7160(11)	7479(12)
C(23′)[d]	2836	4527	8360	B(212)	13(14)	6860(18)	8449(17)

[a] Site occupancy 0.802(4). [b] Site occupancy 0.859(4). [c] Site occupancy 0.198(4). [d] Site occupancy 0.141(4).

$[Pt(^{13}C_2H_5)(dbpp)]BF_4$. A solution of complex **3d** (0.079 g, 0.9 mmol) in CD_2Cl_2 (0.4 cm^3) in an NMR tube was frozen at 77 K and degassed; $^{13}C_2H_4$ (1 mmol) was condensed into the tube along with an estimated 0.2 cm^3 Me_2O. The tube was then sealed and stored at ambient temperature for approximately 30 min to allow ethene exchange to take place. The ^{13}C-labelled analogue of **3e** was prepared in an analogous way.

$[PtH(O_3SCF_3)(dbpp)]$ **4**. Complex **4** formed on allowing a solution of $[PtEt(dbpp)][CF_3SO_3]$ in CH_2Cl_2 to stand for 3 d at 293 K. NMR (CD_2Cl_2, 25 °C): ^1H (hydride moiety only) δ −6.6 [1 H, dd, *J*(PH) 13 and 182, *J*(PtH) 779]; ^{31}P, δ 45.4 [*J*(PtP) 4496] and 34.0 *J*(PtP) 1998 Hz].

Reactions of Complexes **3b**, **3d** *and* **3e** *with Acetonitrile and Pyridine*.—Complexes **3b** and **3d** (*ca.* 0.150 g) were separately dissolved in CD_3CN or C_5D_5N (0.5 cm^3) and the resulting solution transferred to an NMR tube so that the progress of the reaction could be monitored. Complex **3e** (*ca.* 0.15 g) was dissolved in CD_2Cl_2 (0.5 cm^3) and kept at 195 K; CD_3CN (*ca.* 80 μl) was added directly to the cooled sample which was then placed in the previously cooled probe of the NMR instrument.

Crystal Structure Determinations for Complexes **2d**, **3d** *and* **4**.—Many of the details of the structure analyses carried out are listed in Table 8. Crystals of **2d**, **3d** and **4** were grown (colourless blocks, pale cream prisms and colourless cuboids respectively) from Et_2O at *ca.* 0 °C and by the slow vapour diffusion of Et_2O into a CH_2Cl_2 solution of the complex for the last two. The crystal chosen for study was sealed under N_2 in a thin-walled glass capillary tube for diffractometry. Cell dimensions for each analysis were determined from the setting angle values of 42, 37 and 15 centred reflections respectively. Diffracted intensities (θ–2θ scans for **2d** and **4**, and Wyckoff ω scans for **3d**) were collected on Nicolet R3m four-circle diffractometers for a unique volume of reciprocal space using graphite-monochromated Mo-Kα X-radiation ($\bar{\lambda}$ = 0.710 69 Å). Three check reflections remeasured after every 50 ordinary data showed no crystal decay but ±4 and ±5% drifts for **3d** and **4**, and 15% decay for **2d**, over the period of data collection; appropriate corrections were therefore applied. After deletion of these check intensity data, averaging of duplicate and equivalent measurements was carried out and systematic absences were deleted; of the unique data remaining, only those with $F \geqslant n\sigma(F)$ (see Table 8) were used in the solution and refinement of the structures. Corrections for Lorentz, polarization, and X-ray absorption effects were applied. The latter correction was based on a semiempirical method using azimuthal scan data (294, 364 and 499 such data for **2d**, **3d** and **4** respectively).

The Laue group for the diffraction data for complex **3d** is rather close to *mmm*, and the metric symmetry likewise is very close to orthorhombic [refined angles were α = 90.005(14), β = 90.046(13), γ = 90.011(13)°]. Oscillation photographs taken

Table 12 Atomic coordinates (× 10^4) for complex **4**

Atom	*x*	*y*	*z*
Pt	1944(1)	2438(1)	0
P(1)	2794(1)	2328(3)	−675(3)
P(2)	1400(1)	841(3)	−1038(3)
S	1154(1)	3741(3)	1714(3)
F(1)	277(4)	4285(13)	2815(8)
F(2)	79(4)	4164(21)	1334(11)
F(3)	236(7)	2126(16)	2081(15)
O(1)	1172(3)	2813(10)	842(7)
O(2)	1236(4)	5335(8)	1570(7)
O(3)	1449(4)	3122(10)	2513(8)
C(1)	3339(4)	1377(13)	120(11)
C(2)	3062(7)	−98(19)	506(14)
C(3)	3887(6)	912(20)	−376(12)
C(4)	3486(8)	2326(17)	1017(11)
C(5)	3059(6)	4304(14)	−1083(13)
C(6)	3057(7)	5451(16)	−275(18)
C(7)	2643(7)	4813(20)	−1845(15)
C(8)	3665(7)	4243(19)	−1491(18)
C(9)	2827(6)	1143(15)	−1753(9)
C(10)	2335(7)	1039(25)	−2378(11)
C(11)	1839(6)	38(17)	−2022(10)
C(12)	1126(5)	−959(13)	−411(10)
C(13)	879(10)	−2107(16)	−1127(15)
C(14)	1630(6)	−1695(21)	61(19)
C(15)	692(8)	−606(18)	315(13)
C(16)	809(5)	1944(15)	−1677(9)
C(17)	399(10)	2620(22)	−976(21)
C(18)	1056(8)	3187(27)	−2225(18)
C(19)	466(9)	1034(27)	−2396(18)
C(20)	410(7)	3586(23)	2000(15)

about each of the crystallographic axes showed minor deviation from mirror symmetry for the *a* and *c* axes but none for the *b* axis. Furthermore the merging *R* for the observed data under *mmm* symmetry is 0.123; this compares with 0.032 under 2/*m* symmetry. The crystal system was therefore assigned as monoclinic. The diffracted intensities show pronounced pseudo-C centring, only 2057 (out of 6257) reflections with $h + k = 2n + 1$ having $I > 3\sigma(I)$, and the mean $I/\sigma(I)$ for all such reflections being only 3.9. The space group was assigned on the rather ambiguous evidence of the systematic absences (there are very few violations of *a*, *c* or *n* glide conditions for reflections *h*0*l*), and confirmed by successful structure solution and refinement as below. Visual inspection of the data-collection crystal using a polarizing microscope showed no evidence for twinning, although this cannot be taken as proof positive that twinning is not present and responsible for the apparent disorder. We note that in other complexes containing the dbpp ligand similar disorder has been observed.

The structure of complex **3d** was solved by direct and Fourier methods and refined with the molecular cations and anions lying in general positions. There are two crystallographically independent cations and two independent anions in the structure. Both the cations are subject to a partial two-fold site disorder about a pseudo-centre of inversion near the geometric centre of the molecule. This disorder was modelled by assigning the platinum, $(CH_2)_3$, and ethyl carbon atoms occupancy *x* and including second positions for these atoms of occupancy $(1 - x)$, located in Fourier difference syntheses, related by the pseudo-inversion centre. The phosphorus and *tert*-butyl atoms were treated as full occupancy atoms, although each atom of these groups presumably occupies two very slightly separated sites. Occupancy parameters *x* refined to 0.802(4) and 0.859(4) for cations 1 and 2 respectively. The anions were also disordered in the sense that no carbon sites could be definitely located; all cage atoms of the anions were therefore assigned as boron. All full or high-occupancy non-hydrogen atoms, and the low-occupancy platinum atoms [Pt(1′), Pt(2′)], were assigned anisotropic displacement parameters and refined without positional constraints. The low-occupancy carbons [C(11′)–C(15′), C(21′)–C(25′)] were placed in fixed positions and assigned fixed isotropic displacement parameters (0.05 $Å^2$). All hydrogen atoms were constrained to idealized geometries (C–H 0.96 Å, B–H 1.10 Å) and assigned fixed isotropic displacement parameters (0.08 $Å^2$). No hydrogens were assigned to the ethyl carbons or to the low-occupancy ethyl or $(CH_2)_3$ groups. At convergence this model resulted in ten carbon atoms having non-positive-definite anisotropic displacement parameters [C(12)–C(15), C(110), C(115), C(118), C(121), C(26), C(213)] as a consequence of the incomplete modelling of the disorder present in the structure. Although the final goodness of fit (*S*) and the agreement between independent molecules are satisfactory, the disorder affects the entire cation, and in particular the metal and ethyl atomic sites; as a result care should be taken not to overinterpret the bond lengths and angles reported.

The structures of complexes **2d** and **4** were solved by conventional heavy-atom methods, and successive Fourier difference syntheses were used to locate all non-hydrogen atoms, which were refined with anisotropic displacement parameters. The central atom of the dbpp ligand is disordered in **2d**, occupying two positions [C(6) and C(6′)] in the ratio 0.64(1):0.36(1). The hydrogen atoms on the ethyl groups of **2d** and the of hydride ligand in **4** were directly located in Fourier difference syntheses and their positions were refined (with the C–H bonds for the ethyl groups forced to be close to 0.96 Å). All other hydrogen atoms were included at calculated positions (C–H 0.96 Å) with fixed isotropic thermal parameters (except for the ethyl hydrogens in **2d** whose *U* values were refined without constraints). The absolute structure given for **4** was assigned on the basis of an η refinement;[19] the value of η refined to 0.29(6) which is consistent with the given structure although not unambiguously so.

Refinement by full-matrix least squares on *F* with a weighting scheme of the form $w = [\sigma^2(F) + g|F|^2]^{-1}$ [where $\sigma_c^2(F_o)$ is the variance in F_o due to counting statistics and $g = 0.0005$] gave satisfactory analyses of variance and converged to the residuals listed in Table 8. The final electron-density difference syntheses showed no peaks $\geqslant 0.7, 1.1, 1.0$ or $\leqslant -1.1, -0.2, -0.9$ e $Å^{-3}$ for **2d**, **3d** and **4** respectively. Calculations were performed using programs written by Sheldrick.[20] Complex neutral-atom scattering factors were taken from ref. 21. Tables 10–12 report the positional parameters for the non-hydrogen atoms of **2d**, **3d** and **4** respectively.

Additional material available from the Cambridge Crystallographic Data Centre comprises H-atom coordinates, thermal parameters and remaining bond lengths and angles.

Acknowledgements

We thank the SERC for support and Dr. A. D. Redhouse and S. A. Lister, University of Salford, for preliminary work on the X-ray crystallographic determination of [PtEt(dbpp)][$CB_{11}H_{12}$].

References

1 M. Brookhart, M. L. H. Green and L.-L. Wong, *Prog. Inorg. Chem.*, 1988, **36**, 1.
2 N. Carr, B. J. Dunne, A. G. Orpen and J. L. Spencer, *J. Chem. Soc., Chem. Commun.*, 1988, 926; N. Carr, B. J. Dunne, L. Mole, A. G. Orpen and J. L. Spencer, *J. Chem. Soc., Dalton Trans.*, 1991, 863.
3 L. Mole, J. L. Spencer, N. Carr and A. G. Orpen, *Organometallics*, 1991, **10**, 49.
4 H. C. Clark and M. J. Hampden-Smith, *J. Am. Chem. Soc.*, 1986, **108**, 3829.
5 H. Gunter, *Angew. Chem., Int. Ed. Engl.*, 1972, **11**, 861.
6 E. G. Lundquist, K. Folting, W. E. Streib, H. C. Huffman, O. Eistenstein and K. G. Caulton, *J. Am. Chem. Soc.*, 1990, **112**, 855; R. Benn and A. Rufinska, *J. Organomet. Chem.*, 1982, **238**, C27; J. W. Fitch, E. B. Ripplinger, B. A. Shoulders and S. D. Sorey,

J. Organomet. Chem., 1988, **352**, C25; S. Zobl-Ruh and W. von Philipsborn, *Helv. Chim. Acta*, 1981, **64**, 2378; M. Brookhart, A. F. Volpe, jun. and D. M. Lincoln, *J. Am. Chem. Soc.*, 1990, **112**, 5634.
7 D. L. Thorn and R. Hoffmann, *J. Am. Chem. Soc.*, 1978, **100**, 2079.
8 M. Brookhart, D. M. Lincoln, A. F. Volpe, jun. and G. F. Schmidt, *Organometallics*, 1989, **8**, 1212.
9 L. E. Crascall, S. A. Lister, A. D. Redhouse and J. L. Spencer, *J. Organomet. Chem.*, 1990, **394**, C35.
10 G. F. Schmidt and M. Brookhart, *J. Am. Chem. Soc.*, 1985, **107**, 1443.
11 R. B. Cracknell, Ph.D. Thesis, University of Bristol, 1986.
12 L. E. Crascall and J. L. Spencer, *Inorg. Synth.*, 1990, **28**, 126.
13 H. C. Clark and L. E. Manzer, *J. Organomet. Chem.*, 1973, **59**, 411.
14 A. A. del Paggio, R. A. Andersen and E. L. Mutterties, *Organometallics*, 1987, **6**, 1260 and refs. therein.
15 K. Isslieb and A. Tzsach, *Chem. Ber.*, 1959, **92**, 118.
16 C. J. Moulton, Ph.D. Thesis, University of Leeds, 1976.
17 A. R. Siedle and R. A. Newmark, *J. Am. Chem. Soc.*, 1984, **106**, 1510.
18 T. Jelinek, J. Plesek, S. Hermanek and B. Stibr, *Collect. Czech. Chem. Commun.*, 1986, **51**, 819.
19 D. Rogers, *Acta Crystallogr., Sect. A*, 1981, **37**, 734.
20 G. M. Sheldrick, SHELXTL-PLUS, Revision 2.4, University of Göttingen, 1988.
21 *International Tables for X-Ray Crystallography*, Kynoch Press, Birmingham, 1974, vol. 4.

Received 13*th March* 1992; *Paper* 2/01357F